water

MDPI

Article

Efficiency Determination and Mechanism Investigation of Autotrophic Denitrification Strain F1 to Promote Low-Carbon Development

Fang-Kai Qin [1,2], Si-Zhuo Wan [1], Bing-Yin Liu [1], Ru Wang [1,*] and Ping Zheng [3]

[1] Shaanxi Key Lab of Environmental Engineering, Xi'an University of Architecture and Technology, Xi'an 710055, China
[2] XAUAT UniSA An De College, Xi'an University of Architecture and Technology, Xi'an 710055, China
[3] Department of Environmental Engineering, College of Environmental & Resource Science, Zhejiang University, Yuhangtang Road 866, Hangzhou 310058, China
* Correspondence: r.wang@xauat.edu.cn

Abstract: *Shewanella* sp. strain F1, isolated from a lab-scale Fe(II)−dependent anaerobic denitrifying reactor, could reduce nitrate by oxidizing Fe(II). Its nitrate reduction rate and Fe(II) oxidation rate were 0.48 mg/(L·h) and 5.05 mg/(L·h) at OD_{600} of 0.4786 with a five-fold diluent. *Shewanella* sp. was popular in Fe(III) reduction. Fewer studies about its ability for Fe(II) oxidation are available. The low pH was determined to be the switch for *Shewanella* sp. strain F1 to perform Fe(III) reduction or Fe(II) oxidation. Even under a low pH, the produced Fe(III) precipitated around cells from iron encrustation. By observation of the morphologies of strain F1, two corresponding microbial mechanisms were proposed. One was named Cyc 2−based Fe(II)-dependent denitrification, in which Fe(II) was oxidized by Cyc 2 in the outer cell membrane, and the produced Fe(III) precipitated on the cell wall surface to form tiled iron encrustation. The other was named Cyc 1−based Fe(II)−dependent denitrification, in which Fe(II) was oxidized on the existing iron precipitation on the cell wall surface to form towery iron encrustation, and the electron was transported to Cyc 1 in the periplasm. The efficiency determination and mechanism investigation of strain F1 will promote the development of autotrophic denitrification technology and meet the requirement of a low−carbon policy.

Keywords: Fe(II)−dependent autotrophic denitrification; *Shewanella*; denitrifying activity; pH effects; autotrophic denitrifying mechanism

check for updates

Citation: Qin, F.-K.; Wan, S.-Z.; Liu, B.-Y.; Wang, R.; Zheng, P. Efficiency Determination and Mechanism Investigation of Autotrophic Denitrification Strain F1 to Promote Low-Carbon Development. *Water* **2022**, *14*, 3353. https://doi.org/10.3390/w14213353

Academic Editors: Stefano Papirio and Marco Guida

Received: 23 August 2022
Accepted: 18 October 2022
Published: 22 October 2022

Publisher's Note: MDPI stays neutral with regard to jurisdictional claims in published maps and institutional affiliations.

Copyright: © 2022 by the authors. Licensee MDPI, Basel, Switzerland. This article is an open access article distributed under the terms and conditions of the Creative Commons Attribution (CC BY) license (https://creativecommons.org/licenses/by/4.0/).

1. Introduction

Nitrate, as one of the most common pollutants in underground and surface water, may cause serious environmental problems and great public health risks [1]. It is necessary to remove nitrate from water bodies [2]. In the traditional denitrification process, organics are necessary as electron donors, thus increasing the cost and meanwhile generating CO_2, which goes against the aims of the low−carbon economy. Recently, an autotrophic denitrification process with Fe(II) as an electron donor to reduce nitrate in low C/N ratio wastewater has attracted much attention, because (1) it is economical as ferrous salt is much cheaper than organics, e.g., methanol and acetate, (2) it is environmentally friendly because its product is ferric salt rather than greenhouse gas, and (3) its product could be used as a precipitant to remove phosphate and arsenate from wastewater [3–5]. As a new and valuable bioprocess, Fe(II)−dependent autotrophic denitrification is a significant discovery for environmental engineering.

Fe(II)−dependent autotrophic denitrification had been carried out in lab-scale reactors and the volumetric removal rate reached 0.70 kg-N/(m^3·d) [6–8]. To improve the efficiency and reveal the autotrophic denitrification mechanism, pure culture should be isolated and characterized. As was reported, Fe(II)−dependent autotrophic denitrification strains were

distributed widely in *Acidovorax*, *Dechloromonas*, *Paracoccus*, and *Pseudogulbenkiania* [9–11]. However, no information about the autotrophic denitrification mechanism is available.

Therefore, several strains were isolated from the Fe(II)−dependent autotrophic denitrification reactor in our pre-experiments. Among them, strain F1 was chosen for further study as it showed remarkable denitrification activity with Fe(II) as the electron donor. Strain F1 was identified as *Shewanella* sp. However, to our knowledge, *Shewanella* sp. was popular for its ability to reduce Fe(III) and its contribution to the Fe cycle [12–14]. Few reports of their ability to oxidize Fe(II) are available.

Based on the above, first of all, the phenomenon of strain F1 to oxidize Fe(II) and reduce nitrate should be re−verified. The Fe(II) oxidation and nitrate reduction rates should be calculated by Haldane modeling. Then morphological observations on strain F1 cells should be performed to reveal the mechanisms. All results obtained will support the development of Fe(II)−dependent autotrophic denitrification technology, and achieve carbon zero during the denitrification process.

2. Materials and Methods

2.1. Shewanella sp. Strain F1

In total, 7 strains were isolated from a lab−scale Fe(II)−dependent autotrophic denitrification reactor by streak plate method. Among them, strain F1 showed the highest denitrification activity with Fe(II) as an electron donor (Figure S1); thus, the following experiments were carried out by strain F1. By 16s rRNA sequencing analysis, strain F1 was classified into *Shewanella* sp. The GenBank accession number of *Shewanella* sp. strain F1 was KT932999 (Figure S2, noting that the strain was named strain NF−1 in GenBank). Figure S3 showed the detailed morphology characteristics of strain F1. Its colonies presented milk white, spheroidal with a diameter of about 0.7 mm, smooth, convex, and with irregular edges after cultivating for 5 days. Gram test showed that strain F1 was Gram−negative.

For all experiments, a cell suspension of strain F1 was used to make sure equal biomass was added for parallel tests. Cells on the solid medium were washed with sterile water (three times) and collected into a centrifuge tube to be stored at 4 °C as the cell suspension.

2.2. Chemicals and Media

To cultivate the *Shewanella* sp. strain F1, the electron donor was supplied in the form of $FeSO_4 \cdot 7H_2O$, while the electron acceptor was supplied in the form of $NaNO_3$. The chemicals in this experiment were of analytical grade and purchased from Sinopharm Chemical Reagent Co., Ltd., Beijing, China.

The basal medium was shown in Table 1. The pH of the medium was regulated to 6.2 ± 0.2 by adding NaOH (1 M) and HCl (1 M). The cultivation of strain F1 both on the solid medium and in the liquid medium was performed in the anaerobic incubator statically at 30 °C.

Table 1. Composition of the basal medium.

Component	Concentration	Component	Concentration
$NaNO_3$	0.3 g/L	$FeSO_4 \cdot 7H_2O$	5 g/L
$NaHCO_3$	2.5 g/L	$MgSO_4 \cdot 7H_2O$	0.5 g/L
$CaCl_2 \cdot 2H_2O$	0.01 g/L	$(NH_4)_2SO_4$	0.28 g/L
KH_2PO_4	0.25 g/L	EDTA	3.00 mg/L
$Na_2MoO_4 \cdot 2H_2O$	0.036 mg/L	H_3BO_3	0.010 mg/L
$CoCl_2 \cdot 6H_2O$	0.19 mg/L	$NiCl_3 \cdot 6H_2O$	0.024 mg/L
$MnCl_2 \cdot 2H_2O$	0.50 mg/L	$CuCl_2 \cdot 2H_2O$	0.010 mg/L
$ZnCl_2$	0.07 mg/L		

2.3. Morphology Observation

The morphology of the bacterial colony on Petri dishes was observed by a stereoscope (Carl Zeiss AG, Berlin, Germany). A Gram staining test was performed under the aseptic

condition and examined under an optical microscope (Leica, Berlin, Germany). The surface morphology of a single cell was observed by a field emission scanning electron microscope (FESEM) (Hitachi, Tokyo, Japan), and the profile morphology of a single cell was observed by a transmission electron microscope (TEM) (Gtontorn, NJ, USA). Moreover, in view of the specificity of iron−oxidizing bacteria, an energy−dispersive spectrometer (EDS) (Arun, Oxford, UK) was used to determine the extracellular substance.

All bio-samples for morphology observations were collected and stored in glutaric dialdehyde solution at 4 °C. Further treatment and observation were delegated to the Analysis Center of Agrobiology and Environmental Sciences, Zhejiang University.

2.4. Determination of the Denitrification Activity

To determine the Fe(II)−dependent autotrophic denitrification activity of *Shewanella* sp. strain F1, batch experiments were performed in serum bottles. All bottles with the medium were aerated with argon gas for 10 min and sterilized to get rid of oxygen as well as microbes. The dilution ratio was 1:20. All operations were sterile, and bottles were cultivated in an Electrotek anaerobic workstation at 32 °C. Dividing the removed nitrate (and Fe(II)) by the reaction time, the nitrate reduction (and Fe(II) oxidation) rate was calculated.

Further, the effects of the substrate concentration on the activity of strain F1 were studied. The gradient nitrate–nitrogen concentration was 21, 42, 63, 84, 105, 147, or 210 mg/L, while the gradient Fe(II) concentration was 420, 840, 1260, 1680, 2100, 2940, or 4200 mg/L. For each concentration, a parallel group was set, and the concentrations of NO_3^-−N (and Fe(II)) were tested after 24 h. The NO_3^-−N reduction rate and Fe(II) oxidation rate were calculated as described above. The Haldane model was used to fit the data to see the effects of substrate concentration on nitrate reduction rate and Fe(II) oxidation rate [15] (Equation (1)):

$$r_i = \frac{r_{max}}{1 + \frac{K_m}{[S]} + \frac{[S]}{K_i}} \quad (1)$$

where r_i is the removal rate (mg/(L·h)), r_{max} is the maximum removal rate (mg/(L·h)), S is the substrate concentration (mg/L), K_m is the half−rate constant (mg/L), and K_i is the half-inhibition constant (mg/L).

2.5. Effects of Initial pH

Batch experiments were performed in serum bottles to determine the effects of initial pH on the Fe(II)−dependent autotrophic denitrification activity. Bottles with the medium were purged with argon gas for 10 min to maintain anaerobic conditions. The bacteria suspension was inoculated into bottles at a dosage of 5% (v/v) by a sterile operation. The gradient initial pH was set to 5.4, 5.8, 6.2, 6.6, or 7.0 using 1 M HCl and 1 M NaOH. The concentrations of nitrate and Fe(II) were tested after 24 h. The GaussAmp model (Equation (2)) was used to fit the data to determine the optimal initial pH [16]:

$$r = y_0 + r_{max} e^{\frac{-2(pH - pH_m)^2}{w}} \quad (2)$$

where r is the determined nitrate/Fe(II)removal rate (μg/h), y_0 is the basal activity value (μg/h), r_{max} is the maximum removal rate at different initial pH (μg/h), pH is the initial pH value, pH_m is the optimal initial pH value, and w is the reaction coefficient.

2.6. Chemical Analysis

All the samples were analyzed immediately after sampling. The concentrations of nitrate–nitrogen and Fe(II) were determined according to standard methods [17]. The pH values were determined by an S20K pH meter (Mettler Toledo, Geneva, Switzerland). The OD_{600} value of cell suspension was determined by the spectrophotometer (Shimadzu, Tokyo, Japan) at 600 nm.

3. Results

3.1. The Specific Denitrification Activity of Shewanella sp. Strain F1

A batch test was performed to determine the Fe(II)−dependent autotrophic denitrification activity of *Shewanella* sp. strain F1. Both nitrate reduction and Fe(II) oxidation by *Shewanella* sp. strain F1 followed first-order kinetics (Figure 1A,B). When the OD_{600} was 0.4786 with a five−fold diluent, the nitrate reduction rate was 0.48 mg/(L·h) and the Fe(II) oxidation rate was 5.05 mg/(L·h). Fitted with the first-order kinetics, the rate constant of nitrate reduction and Fe(II) oxidation by *Shewanella* sp. strain F1 was 0.0089 h^{-1} and 0.0085 h^{-1}, respectively. The Fe(II)−dependent autotrophic denitrification activity of *Shewanella* sp. strain F1 was much higher than that of reported strains, e.g., *Pseudogulbenkiania* strain 2002, *Microbacterium* strain W5, and *Citrobacter freundii* strain PXL1 [11,18,19]. This remarkable activity was probably because strain F1 was isolated from the high−rate lab-scale Fe(II)−dependent autotrophic denitrification reactor.

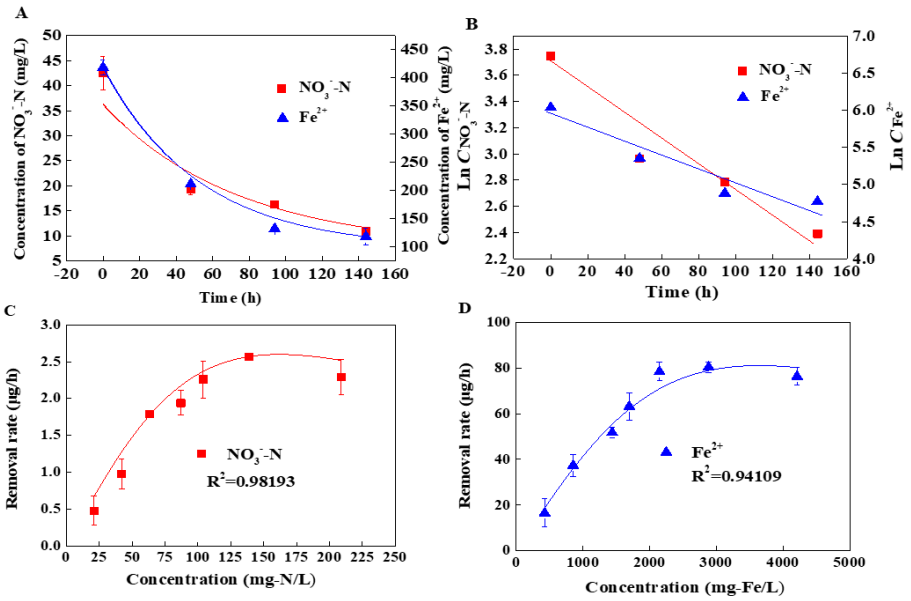

Figure 1. Nitrate reduction and Fe(II) oxidation activities of *Shewanella* sp. strain F1. (**A**) The decrease of nitrate and Fe(II) concentration along with cultivation time. (**B**) The first−order kinetics fitting of nitrate reduction and Fe(II) oxidation rate by strain F1. (**C**) The nitrate reduction rate by strain F1 at different nitrate concentrations. (**D**) The Fe(II) oxidation rate by strain F1 at different Fe(II) concentrations.

The Fe(II)−dependent autotrophic denitrification activity of *Shewanella* sp. strain F1 varied at different substrate concentrations (Figure 1C,D). When the initial nitrate concentration ranged from 21 to 147 mg N/L, the nitrate reduction rate went from 0.45 to 2.56 mg N/(L·h). When the initial nitrate concentration increased to 210 mg N/L, the nitrate reduction rate was inhibited and decreased to 2.31 mg N/(L·h). The Fe(II) oxidation rate shared the same trend as the nitrate reduction rate. When the initial Fe(II) concentration ranged from 420 mg to 2940 mg Fe/L, the Fe(II) oxidation rate went from 15.37 to 81.94 mg Fe/(L·h). When the initial Fe(II) concentration increased to 4200 mg Fe/L, the Fe(II) oxidation rate was inhibited and decreased to 77.40 mg Fe/(L·h). Fitted with the Haldane model (Equation (1)), the maximum removal rate (v_{max}), the half−rate constant (K_m), and the half−inhibition constant (K_i) of nitrate were 2.64 mg N/(L·h), 61.25 mg N/L, and 349.78 mg N/L, respectively. Meanwhile, the v_{max}, K_m, and K_i of Fe(II) were 81.94 mg Fe/(L·h), 942.93 mg Fe/L, and 7811.40 mg Fe/L, respectively (Figure 1). *Shewanella* sp. strain F1 has broad prospects to be applied as an optimal inoculum for autotrophic denitrification technology.

3.2. The Effects of pH on the Denitrification Activity of Shewanella sp. Strain F1

Figure 2A,B illustrate the autotrophic denitrification activity by *Shewanella* sp. strain F1 at different pH values. Data at pH 8.2 are not shown as Fe(II) precipitated as soon as it was added into the reaction system. Little nitrate reduction was observed at pH 7.2, but the decrease in Fe(II) was remarkable. The decrease in Fe(II) at pH 7.2 was caused by chemical precipitation rather than bio-oxidation. *Shewanella* sp. strain F1 had better activity at pH 6.2 than at pH 5.2, because the neutral pH condition benefited the denitrification process [20].

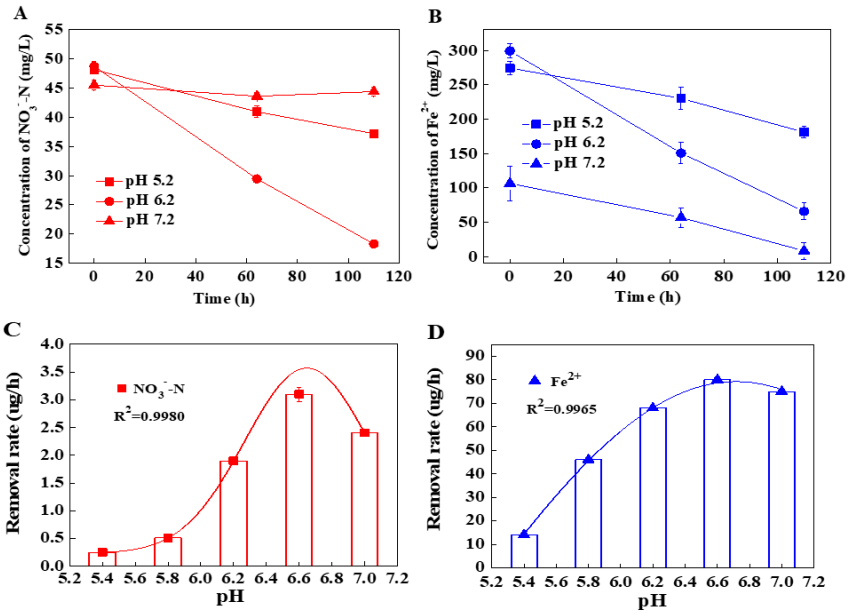

Figure 2. Effects of initial pH on the activity of *Shewanella* sp. strain F1. (**A**) The nitrate reduction activity along with cultivation time. (**B**) The Fe(II) oxidation activity along with time. (**C**) The removal rate of nitrate−nitrogen under different initial pHs. (**D**) The removal rate of Fe(II) under different initial pHs.

The pH affected *Shewanella* sp. strain F1's ability to perform Fe−(II)dependent autotrophic denitrification. A range of pH values was set to determine the optimal pH for strain F1 to reduce nitrate and oxidize Fe(II). The results are shown in Figure 2C,D. In the range of tested pH values, both the nitrate reduction rate and Fe(II) oxidation rate showed peak values, and the peak values were obtained when the initial pH was 6.6. When the initial pH was lower than 6.6, both the nitrate reduction rate and Fe(II) oxidation rate increased to their peak values, then began to decrease when the initial pH exceeded 6.6. Fitted by the GaussAmp model (Equation (2)), the optimal pH for nitrate reduction and Fe(II) oxidation was 6.66 and 6.69, respectively (Figure 2C,D).

3.3. The Morphology Observation of Shewanella sp. Strain F1

Figure 3 shows the morphological characteristics of strain F1. When cultivating strain F1 with nitrate and ferrous salts at pH 6.6, some attachments were observed on the cell wall surface. They were tiled or towery. The tiled attachment formed a layer to cover the cell, while the towery attachment accumulated on the specific point on the cell wall surface.

The attachment on the cell wall surface was speculated to be ferric/ferrous oxyhydroxide [21–24]. To ascertain the composition of attachments, EDS was used and the results are shown in Figure 4. The major elements on the cell wall surface were carbon, oxygen, and iron, in descending order (Figure 4C–E). Carbon was distributed evenly in the view, while oxygen and iron were distributed only on the cell wall surface. Iron and oxygen accounted for only a small part compared with carbon, because the conductive adhesive that acted as the carrier for FESEM samples was made of carbon. From Figure 4, we concluded that the attachment on the cell wall surface mainly consisted of iron and oxygen. The product

of Fe(II) oxidation, Fe(III), tended to precipitate on the cell wall surface as soon as it was produced because of the high pH (~6.2). The precipitated Fe(III) formed attachments to cells and will be referred to as iron encrustation hereafter.

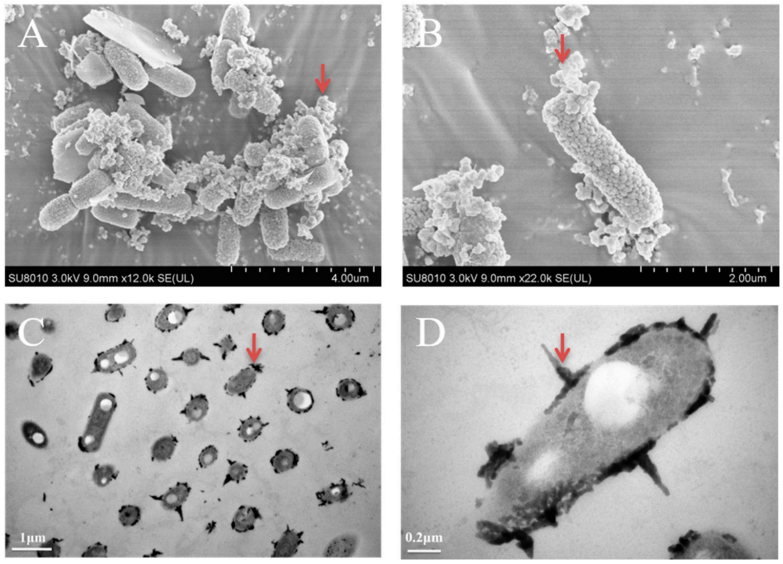

Figure 3. Morphological characteristics of strain F1. (**A**,**B**) Surface morphology of cell wall by FETEM. (**C**,**D**) Profile morphology of the cell wall by TEM. Arrows refer to the iron encrustation.

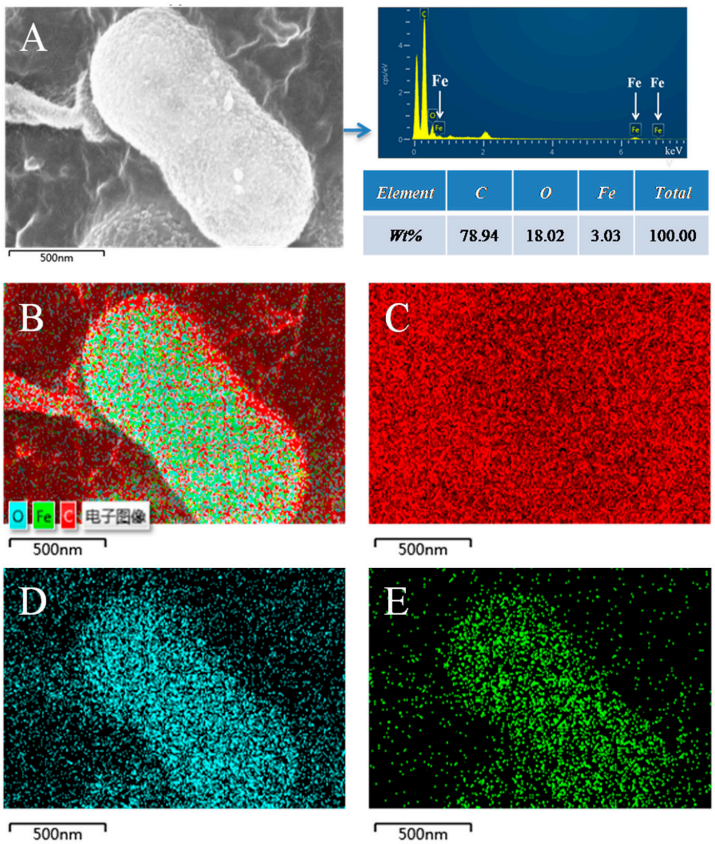

Figure 4. FESEM images of strain F1 and the surface contents analysis by EDS. (**A**) The view of the targeted cell and the composition of main elements. (**B**) Overlay chart of the distribution of carbon, oxygen, and iron. (**C**) Distribution of carbon in the view. (**D**) Distribution of oxygen in the view. (**E**) Distribution of iron in the view.

4. Discussion

4.1. The Switch for Shewanella sp. Strain F1 to Perform Autotrophic Denitrification

In recent decades, *Shewanella* spp. have received attention for their role in the iron cycle [25–27]. However, *Shewanella* spp. were only deemed to reduce Fe(III) [28–30]. Few reports of their ability to oxidize Fe(II) are available. From the results in Section 3.1, we see that *Shewanella* sp. strain F1 possesses remarkable Fe(II)−dependent autotrophic denitrification activity. That indicates that the strain could oxidize Fe(II) and reduce nitrate effectively.

As reported, the *Shewanella* sp. prefer to live in alkaline or circumneutral pH environments, and only in these environments could they reduce Fe(III) [31,32]. In this study, *Shewanella* sp. strain F1 was tested in weakly acidic conditions (pH 6.2) and it oxidized Fe(II). As shown in Section 3.2, obvious Fe(II)−dependent autotrophic denitrification activity was only observed at pH 5.2 and 6.2. Thus, the pH was speculated to be the switch for *Shewanella* sp. strain F1 to oxidize Fe(II) rather than reduce Fe(III). The reason might be that the low pH inhibited the activity of iron reductase, and the microorganism had to exploit other ways to obtain energy. However, further studies need to be carried out to prove this hypothesis.

4.2. The Conceptual Mechanism of Shewanella sp. Strain F1 to Perform Autotrophic Denitrification

From Section 3.3, two kinds of iron encrustation were observed around cells, in tiled or towery shapes (Figure 3). From our previous publications and literature by other research groups [19–22,33,34], the iron encrustations were mainly ferric compounds with a small part of ferrous compounds. From Figure 3C,D, for most of the strain F1 cells, both tiled or towery iron encrustation existed. The iron encrustation affected the nutrient transportation and decreased the activity of strain F1 cells. However, there were still large areas of exposure for each cell, signifying the nutrient transportation was not cut off. Based on the formation of iron encrustation and the electron transport chain of denitrification, two conceptual mechanisms of autotrophic denitrification by *Shewanella* sp. strain F1 are shown in Figure 5. In Figure 5A, which shows the formation of the tiled iron encrustation, the oxidation of Fe(II) to Fe(III) is carried out by a C−type cytochrome (Cyc 2) present in the outer cell membrane [35]. This is called Cyc 2−based autotrophic denitrification. Electrons are transferred to the cytoplasmic membrane through a terminal 'aa_3 cytochrome oxidase', and again to the electron transport chain that supports the downstream denitrification. Molecules that shuttle electrons are Cyc 1 and rusticyanin [36,37]. Figure 5B shows the formation of the towery iron encrustation. Different from the formation of tiled iron encrustation, to form the towery iron encrustation, Fe(II) gives the electron to the iron precipitate and becomes Fe(III) [38,39]. Fe(III) continues precipitating on the iron precipitate. The electron travels to Cyc 1 and participates in the electron transport chain, which supports the denitrification process. This is called Cyc 1−based autotrophic denitrification. Both mechanisms were observed in this study.

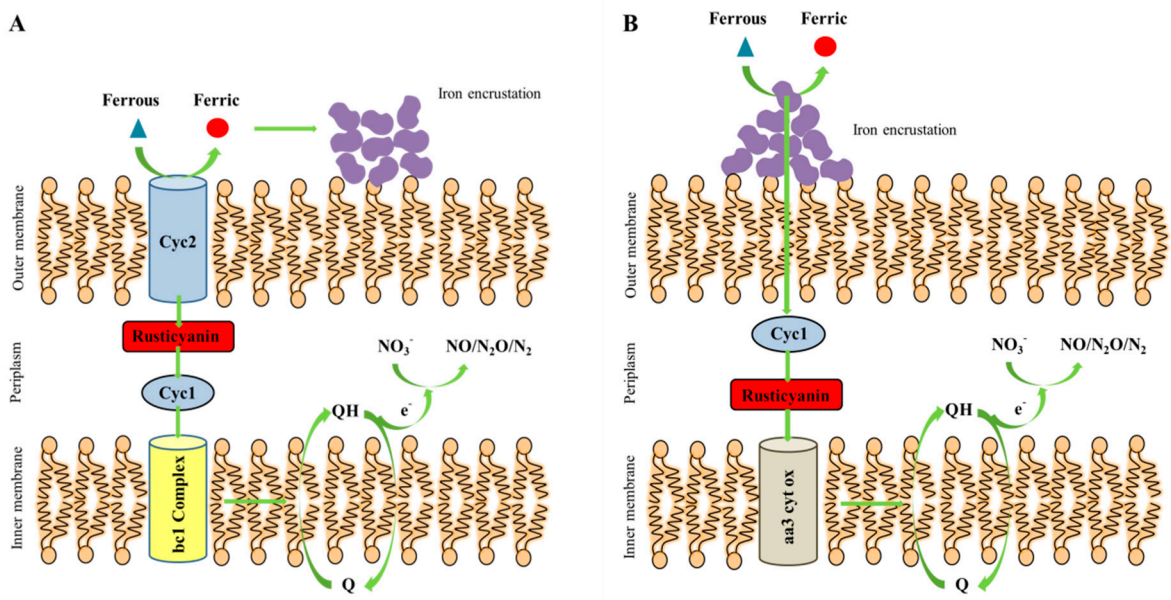

Figure 5. The conceptual autotrophic denitrification mechanisms by *Shewanella* sp. strain F1. The tiled iron encrustation was formed as shown in (**A**), while the towery iron encrustation was formed as shown in (**B**).

5. Conclusions

Shewanella sp. strain F1 showed remarkable autotrophic denitrification activity and could be the optimal seeding sludge for Fe(II)−dependent autotrophic denitrification processes. Differing from the conventional understanding of *Shewanella* sp. being the Fe(III) reducer, *Shewanella* sp. strain F1 showed Fe(II) oxidizing activity with nitrate as the electron acceptor. That may 'clue' new Fe cycles in the lithosphere and biosphere. The pH was determined to be the trigger for *Shewanella* sp. strain F1 to perform Fe(III) oxidation from Fe(II) reduction under batch tests. Further observation and more proving tests should be carried out. Combining the electron transport chain of denitrification and the observed results, Cyc 2−based and Cyc 1−based autotrophic denitrification mechanisms were proposed. Even though the formation of iron encrustation was inevitable, there were still exposed areas for strain F1 cells to transport nutrients, maintaining the activity of nitrate reduction and Fe(II) oxidation. The isolation and efficiency determination of *Shewanella* sp. strain F1, and the corresponding mechanism investigation will promote the development of Fe(II)−dependent autotrophic denitrification technology that meets the requirement of a low−carbon policy.

Supplementary Materials: The following supporting information can be downloaded at: https://www.mdpi.com/article/10.3390/w14213353/s1, Figure S1: The nitrate and ferrous ion removal efficiency of seven isolated strains from the lab-scale reactor; Figure S2: Phylogenetic tree of strain F1. Numbers in parentheses represent the sequences' accession number in GenBank. The number at each branch points is the percentage supported by bootstrap (1000 re-samplings). Bar: 0.5% sequence divergence; Figure S3: Morphological characteristics of strain F1. A: colony morphology by the stereoscope; B: Gram stain observed by the optical microscope.

Author Contributions: Conceptualization, P.Z. and R.W.; methodology, R.W.; software, S.-Z.W.; validation, F.-K.Q. and B.-Y.L.; formal analysis, F.-K.Q. and B.-Y.L.; investigation, S.-Z.W.; resources, R.W. and P.Z.; data curation, R.W.; writing—original draft preparation, F.-K.Q.; writing—review and editing, R.W.; visualization, R.W.; supervision, R.W.; project administration, R.W.; funding acquisition, R.W. and P.Z. All authors have read and agreed to the published version of the manuscript.

Funding: This research was funded by the National Natural Science Foundation of China (grant no. 51808433).

Conflicts of Interest: The authors declare no conflict of interest.

References

1. Kim, T.; Shin, J.; Lee, D.; Kim, Y.; Na, E.; Park, J.; Lim, C.; Cha, Y. Simultaneous feature engineering and interpretation: Forecasting harmful algal blooms using a deep learning approach. *Water Res.* **2022**, *215*, 118289. [CrossRef] [PubMed]
2. Lu, W.; Zhang, Y.; Wang, Q.; Wei, Y.; Bu, Y.; Ma, B. Achieving advanced nitrogen removal in a novel partial denitrification/anammox-nitrifying (PDA-N) biofilter process treating low C/N ratio municipal wastewater. *Bioresour. Technol.* **2021**, *340*, 125661. [CrossRef] [PubMed]
3. Li, X.; Qin, R.; Yang, W.; Su, C.; Luo, Z.; Zhou, Y.; Lin, X.; Lu, Y. Effect of asparagine, corncob biochar and Fe(II) on anaerobic biological treatment under low temperature: Enhanced performance and microbial community dynamic. *J. Environ. Manag.* **2022**, *317*, 115348. [CrossRef]
4. Wang, P.; Li, W.; Ren, S.; Peng, Y.; Wang, Y.; Feng, M.; Guo, K.; Xie, H.; Li, J. Use of sponge iron as an indirect electron donor to provide ferrous iron for nitrate-dependent ferrous oxidation processes: Denitrification performance and mechanism. *Bioresour. Technol.* **2022**, *357*, 127318. [CrossRef] [PubMed]
5. Zhang, M.; Zheng, P.; Abbas, G.; Chen, X. Partitionable-space enhanced coagulation (PEC) reactor and its working mechanism: A new prospective chemical technology for phosphorus pollution control. *Water Res.* **2013**, *49*, 426–433. [CrossRef] [PubMed]
6. Wang, R.; Xu, S.-Y.; Zhang, M.; Ghulam, A.; Dai, C.-L.; Zheng, P. Iron as electron donor for denitrification: The efficiency, toxicity and mechanism. *Ecotoxicol. Environ. Saf.* **2020**, *194*, 110343. [CrossRef]
7. Wang, R.; Yang, C.; Zhang, M.; Xu, S.-Y.; Dai, C.-L.; Liang, L.-Y.; Zhao, H.-P.; Zheng, P. Chemoautotrophic denitrification based on ferrous iron oxidation: Reactor performance and sludge characteristics. *Chem. Eng. J.* **2017**, *313*, 693–701. [CrossRef]
8. Zhang, M.; Zheng, P.; Li, W.; Wang, R.; Ding, S.; Abbas, G. Performance of nitrate-dependent anaerobic ferrous oxidizing (NAFO) process: A novel prospective technology for autotrophic denitrification. *Bioresour. Technol.* **2015**, *179*, 543–548. [CrossRef] [PubMed]
9. Chen, Y.; Li, X.; Liu, T.; Li, F.; Sun, W.; Young, L.Y.; Huang, W. Metagenomic analysis of Fe(II)-oxidizing bacteria for Fe(III) mineral formation and carbon assimilation under microoxic conditions in paddy soil. *Sci. Total Environ.* **2022**, *851*, 158068. [CrossRef] [PubMed]
10. Li, Z.; Peng, Y.; Gao, H. Enhanced long-term advanced denitrogenation from nitrate wastewater by anammox consortia: Dissimilatory nitrate reduction to ammonium (DNRA) coupling with anammox in an upflow biofilter reactor equipped with EDTA-2Na/Fe(II) ratio and pH control. *Bioresour. Technol.* **2020**, *305*, 123083. [CrossRef] [PubMed]
11. Chen, D.; Liu, T.; Li, X.; Li, F.; Luo, X.; Wu, Y.; Wang, Y. Biological and chemical processes of microbially mediated nitrate-reducing Fe(II) oxidation by *Pseudogulbenkiania* sp. strain 2002. *Chem. Geol.* **2018**, *476*, 59–69. [CrossRef]
12. Dong, H.; Zhang, F.; Xu, T.; Liu, Y.L.; Du, Y.; Wang, C.; Liu, T.S.; Gao, J.; He, Y.L.; Wang, X.T.; et al. Culture-dependent and culture-independent methods reveal microbe-clay mineral interactions by dissimilatory iron-reducing bacteria in an integral oilfield. *Sci. Total Environ.* **2022**, *840*, 156577. [CrossRef]
13. Lu, Y.S.; Liu, H.; Huang, X.E.; Xu, L.; Zhou, J.Z.; Qian, G.R.; Shen, J.P.; Chen, X.P. Nitrate removal during Fe(III) bio-reduction in microbial-mediated iron redox cycling systems. *Water. Sci. Technol.* **2021**, *84*, 985–994. [CrossRef]
14. Mateos, G.; Bonilla, A.M.; de Polanco, S.D.; Martinez, J.M.; Escudero, C.; Rodriguez, N.; Sanchez-Andrea, I.; Amils, R. *Shewanella* sp. T2.3D-1.1 a novel microorganism sustaining the iron cycle in the deep subsurface of the Iberian Pyrite Belt. *Microorganisms* **2022**, *10*, 1585. [CrossRef] [PubMed]
15. Zhang, H.; Zhao, K.; Liu, X.; Chen, S.; Huang, T.; Guo, H.; Ma, B.; Yang, W.; Yang, Y.; Liu, H. Bacterial community structure and metabolic activity of drinking water pipelines in buildings: A new perspective on dual effects of hydrodynamic stagnation and algal organic matter invasion. *Water Res.* **2022**, *225*, 119161. [CrossRef] [PubMed]
16. Wang, R.; Wan, S.; Lai, L.; Zhang, M.; Zeb, B.S.; Qaisar, M.; Tan, G.; Yuan, L. Recovering phosphate and energy from anaerobic sludge digested wastewater with iron-air fuel cells: Two-chamber cell versus one-chamber cell. *Sci. Total Environ.* **2022**, *825*, 154034. [CrossRef] [PubMed]
17. Liu, J.; Shentu, H.; Chen, H.; Ye, P.; Xu, B.; Zhang, Y.; Zhang, T. Change regularity of water quality parameters in leakage flow conditions and their relationship with iron release. *Water Research* **2017**, *124*, 353–362. [CrossRef] [PubMed]
18. Su, J.F.; Shao, S.C.; Huang, T.L.; Ma, F.; Yang, S.F.; Zhou, Z.M.; Zheng, S.C. Anaerobic nitrate-dependent iron(II) oxidation by a novel autotrophic bacterium, *Pseudomonas* sp. SZF15. *J. Environ. Chem. Eng.* **2015**, *3*, 2187–2193. [CrossRef]
19. Zhou, J.; Wang, H.; Yang, K.; Sun, Y.; Tian, J. Nitrate removal by nitrate-dependent Fe(II) oxidation in an upflow denitrifying biofilm reactor. *Water Sci. Technol.* **2015**, *72*, 377–383. [CrossRef] [PubMed]
20. Ji, B.; Yang, K.; Zhu, L.; Jiang, Y.; Wang, H.; Zhou, J.; Zhang, H. Aerobic denitrification: A review of important advances of the last 30 years. *Biotechnol. Bioprocess Eng.* **2015**, *20*, 643–651. [CrossRef]
21. Yuan, Z.; Ma, X.; Wang, S.; Yu, L.; Zhang, P.; Lin, J.; Jia, Y. Effect of co-existent Al(III) in As-rich Acid Mine Drainage (AMD) on As removal during Fe(II) and As(III) abiotic oxidation process. *J. Water Process Eng.* **2021**, *44*, 102395. [CrossRef]
22. Wang, H.; Fan, Y.; Zhou, M.; Wang, W.; Li, X.; Wang, Y. Function of Fe(III)-minerals in the enhancement of anammox performance exploiting integrated network and metagenomics analyses. *Water Res.* **2022**, *210*, 117998. [CrossRef] [PubMed]
23. Liu, Y.; Feng, C.; Sheng, Y.; Dong, S.; Chen, N.; Hao, C. Effect of Fe(II) on reactivity of heterotrophic denitrifiers in the remediation of nitrate- and Fe(II)-contaminated groundwater. *Ecotoxicol. Environ. Saf.* **2018**, *166*, 437–445. [CrossRef]

24. Schmid, G.; Zeitvogel, F.; Hao, L.; Ingino, P.; Flötenmeyer, M.; Stierhof, Y.D.; Schröppel, B.; Burkhardt, C.; Kappler, A.; Obst, M. 3-D analysis of bacterial cell-(iron)mineral aggregates formed during Fe(II) oxidation by the nitrate-reducing *Acidovorax* sp. strain BoFeN1 using complementary microscopy tomography approaches. *Geobiology* **2014**, *12*, 340–361. [CrossRef]
25. Huang, X.; Yang, X.; Zhu, J.; Yu, J. Microbial interspecific interaction and nitrogen metabolism pathway for the treatment of municipal wastewater by iron carbon based constructed wetland. *Bioresour. Technol.* **2020**, *315*, 123814. [CrossRef]
26. Li, B.; Cheng, Y.; Wu, C.; Li, W.; Yang, Z.; Yu, H. Interaction between ferrihydrite and nitrate respirations by *Shewanella oneidensis* MR-1. *Process Biochem.* **2015**, *50*, 1942–1946. [CrossRef]
27. Singh, V.K.; Singh, A.L.; Singh, R.; Kumar, A. Iron oxidizing bacteria: Insights on diversity, mechanism of iron oxidation and role in management of metal pollution. *Environ. Sustain.* **2018**, *1*, 221–231. [CrossRef]
28. Zhu, F.; Huang, Y.; Ni, H.; Tang, J.; Zhu, Q.; Long, Z.; Zou, L. Biogenic iron sulfide functioning as electron-mediating interface to accelerate dissimilatory ferrihydrite reduction by *Shewanella oneidensis* MR-1. *Chemosphere* **2022**, *288*, 132661. [CrossRef]
29. Su, J.F.; Guo, D.X.; Huang, T.L.; Bai, X.C.; Lu, J.S.; Wei, L.; He, L. Microbial Community Analysis and Effect of nZVI on Autotrophic Denitrification in a Biological Reactor. *Environ. Eng. Sci.* **2019**, *36*, 564–572. [CrossRef]
30. Wang, X.-N.; Sun, G.-X.; Li, X.-M.; Clarke, T.A.; Zhu, Y.-G. Electron shuttle-mediated microbial Fe(III) reduction under alkaline conditions. *J. Soils Sediments* **2017**, *18*, 159–168. [CrossRef]
31. Jia, R.; Wang, K.; Li, L.; Qu, Z.; Shen, W.; Qu, D. Abundance and community succession of nitrogen-fixing bacteria in ferrihydrite enriched cultures of paddy soils is closely related to Fe(III)-reduction. *Sci. Total Environ.* **2020**, *720*, 137633. [CrossRef] [PubMed]
32. Zhang, M.; Zhangzhu, G.C.; Wen, S.X.; Lu, H.F.; Wang, R.; Li, W.; Ding, S.; Ghulam, A.; Zheng, P. Chemolithotrophic denitrification by nitrate-dependent anaerobic iron oxidizing (NAIO) process: Insights into the evaluation of seeding sludge. *Chem. Eng. J.* **2018**, *345*, 345–352. [CrossRef]
33. Zhang, M.; Zheng, P.; Zeng, Z.; Wang, R.; Shan, X.Y.; He, Z.F.; Abbas, G.; Ji, J.Y. Physicochemical characteristics and microbial community of cultivated sludge for nitrate-dependent anaerobic ferrous-oxidizing (NAFO) process. *Sep. Purif. Technol.* **2016**, *169*, 296–303. [CrossRef]
34. Shi, L.; Rosso, K.M.; Zachara, J.M.; Fredrickson, J.K. Mtr extracellular electron-transfer pathways in Fe(III)-reducing or Fe(II)-oxidizing bacteria: A genomic perspective. *Biochem. Soc. Trans.* **2012**, *40*, 1261–1267. [CrossRef] [PubMed]
35. Pirbadian, S.; Barchinger, S.E.; Leung, K.M.; Byun, H.S.; Jangir, Y.; Bouhenni, R.A.; Reed, S.B.; Romine, M.F.; Saffarini, D.A.; Shi, L.; et al. *Shewanella oneidensis* MR-1 nanowires are outer membrane and periplasmic extensions of the extracellular electron transport components. *Proc. Natl. Acad. Sci. USA* **2014**, *111*, 12883–12888. [CrossRef]
36. Lin, T.; Ding, W.; Sun, L.; Wang, L.; Liu, C.; Song, H. Engineered *Shewanella* oneidensis-reduced graphene oxide biohybrid with enhanced biosynthesis and transport of flavins enabled a highest bioelectricity output in microbial fuel cells. *Nano Energy* **2018**, *50*, 639–648. [CrossRef]
37. Beblawy, S.; Bursac, T.; Paquete, C.; Louro, R.; Clarke, T. Extracellular reduction of solid electron acceptors by *Shewanella oneidensis*. *Mol. Microbiol.* **2018**, *109*, 571–583. [CrossRef]
38. Chen, L.; Wu, Y.; Shen, Q.; Zheng, X.; Chen, Y. Enhancement of hexavalent chromium reduction by *Shewanella oneidensis* MR-1 in presence of copper nanoparticles via stimulating bacterial extracellular electron transfer and environmental adaptability. *Bioresour. Technol.* **2022**, *361*, 127686. [CrossRef] [PubMed]
39. Wang, H.; Zhao, H.; Zhu, L. Structures of nitroaromatic compounds induce *Shewanella oneidensis* MR-1 to adopt different electron transport pathways to reduce the contaminants. *J. Hazard. Mater.* **2020**, *384*, 121495. [CrossRef]